Published in final edited form as:
J Appl Polym Sci. 2011 July ; 121(1): 144–153. doi:10.1002/app.33428.

Post-Polymerization Crosslinked Polyurethane Shape-Memory Polymers

K. Hearon[1,2,3], **K. Gall**[1], **T. Ware**[1], **D. J. Maitland**[2,3], **J. P. Bearinger**[2], and **T. S. Wilson**[2]

[1] School of Materials Science and Engineering, Georgia Institute of Technology, Atlanta, GA, 30332

[2] Physical and Life Science Directorate, Lawrence Livermore National Laboratory, Livermore, CA 94551

[3] Department of Biomedical Engineering, College Station, TX 77843

Abstract

Novel urethane shape-memory polymers (SMPs) of significant industrial relevance have been synthesized and characterized. Chemically crosslinked SMPs have traditionally been made in a one-step polymerization of monomers and crosslinking agents. However, these new post-polymerization crosslinked SMPs can be processed into complex shapes by thermoplastic manufacturing methods and later crosslinked by heat exposure or by electron beam irradiation. Several series of linear, olefinic urethane polymers were made from 2-butene-1,4-diol, other saturated diols, and various aliphatic diisocyanates. These thermoplastics were melt-processed into desired geometries and thermally crosslinked at 200°C or radiation crosslinked at 50 kGy. The SMPs were characterized by solvent swelling and extraction, differential scanning calorimetry (DSC), dynamic mechanical analysis (DMA), tensile testing, and qualitative shape-recovery analysis. Swelling and DMA results provided concrete evidence of chemical crosslinking, and further characterization revealed that the urethanes had outstanding mechanical properties. Key properties include tailorable transitions between 25 and 80°C, tailorable rubbery moduli between 0.2 and 4.2 MPa, recoverable strains approaching 100%, failure strains of over 500% at T_g, and qualitative shape-recovery times of less than 12 seconds at body temperature (37°C). Because of its outstanding thermo-mechanical properties, one polyurethane was selected for implementation in the design of a complex medical device. These post-polymerization crosslinked urethane SMPs are an industrially relevant class of highly processable shape-memory materials.

INTRODUCTION

Shape-memory polymers (SMPs) are being proposed for a diverse set of engineering applications.[1–3] Because SMPs can retain fixed secondary shapes and recover their original shapes upon heating, their applications are often directed at, but are not limited to, the biomedical industry.[2,4–8] For example, an SMP-based suture anchor for graft fixation called Morphix® received FDA approval in February 2009 and has recently been implanted into humans for the first time.[9] An SMP-based interventional microactuator device for treating ischemic stroke[3] is currently being subjected to animal testing at the Texas A&M Institute for Preclinical Studies. SMPs have also received attention for applications outside the medical industry. Raytheon© is currently investigating SMP foams for implementation in thermally-activated wing-deployment systems.[6,10]

Corresponding Author: Thomas S. Wilson, wilson97@llnl.gov.

Although significant progress has been made in the development of new SMPs for engineering applications, difficulties in SMP processing have sometimes occurred because chemically crosslinked SMPs are currently produced in a one-step polymerization of monomers and crosslinking agents.[11–12] Covalently bonded chemically crosslinked SMPs offer numerous advantages over physically crosslinked SMPs, which include superior cyclic recoverable strains, higher rubbery modulus values, and higher toughness values.[13] These thermoset SMPs are traditionally synthesized either by photo-polymerization or heat-curing of liquid monomers.[14–15] The chemical reactions that occur during polymerization often result in significant volume change, which makes complex molding difficult. Thermoset polymers cannot be melted, so traditional thermoplastic processing methods such as injection molding cannot be used to reshape chemically crosslinked SMPs to fix deformities. Without the use of injection molding or other thermoplastic processing techniques, the mass-production of complex SMP-based products is neither economically feasible nor advantageous.

Certain applications demand a shape memory polymer that can be melt-processed as a thermoplastic and then crosslinked during a secondary step to fix its final shape. This idea of inducing chemical crosslinking into thermoplastic polymer chains is not in itself novel: it dates back to the 19th century, when the process of vulcanization was developed by Charles Goodyear.[16] Late 20th Century projects such as those of Le Roy[17] (1982) and Goyert[18] (1988) achieved successful crosslinking of thermoplastic polyurethanes and acrylates using irradiation, and Bezuidenhout, et al. were awarded U.S. Patent 7538163 in 2009 for the development of other chemical mechanisms of post -polymerization urethane crosslinking.[19] In the shape-memory polymers field, Voit, et al. have recently been investigating post-polymerization crosslinking in thermoplastic polyacrylate systems.[20–21] However, none of these works, nor any others to our knowledge, have specifically aimed to apply the concept of post-polymerization crosslinking to the synthesis, characterization, and optimization of the thermo-mechanical properties of polyurethane shape-memory polymers with transition temperatures in the range relevant for biomedical applications. A comparison of traditional chemically crosslinked SMPs and the novel SMPs whose synthesis was attempted in this work is provided in Figure 1. We explored both thermally activated and radiation-induced crosslinking methods.

The objectives of this work were the synthesis and characterization of a novel polyurethane SMP that could be made into a thermoplastic polymer, processed into a complex geometry, and later crosslinked in a final curing step. To achieve these objectives, we synthesized a series of linear, olefinic urethane polymers from 2-butene-1,4-diol, 1,6-hexanediol, 1,8-octanediol, trimethylhexamethylene diisocyanate (TMHDI), and dicyclohexylmethane 4,4′-diisocyanate (DCHMDI). The chemical structures of these monomers are illustrated in Table 1. Monomers were selected which were predicted to produce polymers with glass transitions in the range of 20–80°C. Urethane chemistry was selected because of the high relative thermodynamic stability of the vinyl group in 2-butene-1,4-diol relative to the stability of the isocyanate/diol reaction and in order to incorporate crosslink sites along the chains at fairly uniform intervals. This unsaturated site was predicted to remain unreactive during the initial polymerization and thus be preserved in the polymer backbone. Post-condensation crosslinking was then attempted at or near the unsaturated sites.

Target mechanical properties included a glass transition temperature (T_g) below body temperature (37°C), a sharp glass transition range, a high rubbery modulus, a high strain to failure at T_g, a high recoverable strain, a high recoverable force, and a fast shape recovery time at body temperature. Dynamic Mechanical Analysis (DMA) and solvent extraction experiments were carried out in order to confirm the occurrence of post-polymerization crosslinking and to characterize this novel crosslinking mechanism. Further DMA tests, as

well as DSC, tensile testing, and qualitative shape-recovery analysis experiments were run to evaluate the biomedical relevance of the new urethane materials.

EXPERIMENTAL

Materials and Thermoplastic Sample Preparation

Thermoplastic urethane samples were synthesized from monomers which were predicted to have a potential for post-polymerization crosslinking. Three distinct series of materials were synthesized. Series 1a-1e, was prepared from 2-butene-1,4-diol (95%) and varying ratios of TMHDI, (97%, TCI America), and DCHMDI, (97%, TCI America). Series 1a-1e consisted of 0%, 5%, 10%, 20%, and 30% DCHMDI (overall molar percent). Increasing DCHMDI composition was predicted to raise the T_g. Sample 1f was prepared from TMHDI and 1,4-butanediol (98%) in order to evaluate the effect of the double bond in 2-butene-1,4-diol on crosslinking. Series 2 was prepared from TMHDI and varying ratios of 2-butene-1,4-diol and 1,8-octanediol (98%). Series 2a–2d consisted of 5%, 15%, 20%, and 25% 1,8-octanediol (overall molar percent). Series 3 was prepared from TMHDI and varying ratios of 2-butene-1,4-diol and 1,6-hexanediol (98%). Series 3a–3d consisted 10%, 15%, 20%, and 25% 1,6-hexanediol (overall molar percent). The saturated diols were added to lower the T_g. The chemical compositions of all samples are listed in Table 1.

All chemicals, unless otherwise stated, were purchased from Sigma-Aldrich and used as received. All urethanes were prepared in 50% THF solution (anhydrous, >99.9%) using stoichiometric diisocyante/diol ratios. The isocyanate monomers were stored under dry nitrogen until use to prevent moisture absorption. The stoichiometric diol-diisocyanate solutions were prepared in glass vials. The vials were loosely sealed (to prevent pressure buildup) and were placed in a Thermoline furnace at 60°C under a dry nitrogen atmosphere for 24 hours. The polymer solutions were then poured into polypropylene dishes and placed into a Yamato Benchtop Vacuum Drying Oven at 80°C at 1 torr for 48–144 hours.

After drying under vacuum, the thermoplastic samples were mostly solvent free. The samples were then removed from the polypropylene dishes and pressed to a thickness of 1 mm using a Carver hot press at 150°C for 20–30 seconds. The samples were pressed between Teflon-coated stainless steel plates using a 1 mm-thick square stainless steel spacer.

Preparation of Thermally and Radiation Crosslinked Samples

After the thermoplastic samples were synthesized, they were subjected to heat or radiation in an attempt to induce chemical crosslinking. The samples prepared for thermal crosslinking were put back on the Teflon-coated stainless steel plates and placed in the Yamato vacuum oven at 200°C at 1 torr until the onset of crosslinking was visible. The onset of crosslinking was marked by the failure of bubbles in the samples to evaporate out. After the onset of crosslinking, vacuum was released, and the samples were left under nitrogen at 200°C for 10 hours. Heat crosslinking only yielded testable, thin-film samples for Series I. The 1mm-thick films were laser-cut into DMA and dog bone samples using a Universal Laser Systems CO_2 VeraLaser machine. The heat-crosslinked Series 1 samples were then labeled 1H-a to 1H-e. It is important to note that no thermal initiator was used to induce thermal crosslinking.

Sample 1a was exposed to different temperatures for varying amounts of time in order to evaluate the effects of temperature and heat exposure time on crosslinking. In Series 4, thermoplastic 1a samples (0% DCHMDI) were placed in the oven at 200°C for 1, 2, 3, 4, 6, 8, 10, and 12 hours. Samples were labeled Series 4a, 4b, etc. Another series of thermally crosslinked 0% DCHMDI samples, Series 5, was made from heat exposure 225°C for 2.5, 4, 6, and 8 hours and was labeled Series 5a, 5a, etc. After being pressed to 1mm-thick films, all

thermoplastic samples in Series 1–3 were exposed to electron beam radiation at 50 kGy. Irradiated samples were labeled 1R-a, 2R-a, etc.

Characterization by Swelling and Extraction

In order to determine if the heated and irradiated samples were crosslinked, solvent swelling and extraction experiments were run to determine gel fraction. Swelling experiments were run on all samples in Series 1H and 1R, as well as on select samples in Series 2R and 3R. Since the thermoplastic urethanes were synthesized in 50% THF solution and remained in solution after polymerization, THF was chosen as the solvent for the swelling experiments. 0.5g samples were massed, put in 50:1 THF mixtures in 40 mL glass vials, and heated at 50°C on a J-Kem Scientific Max 2000 reaction block at 150 rpm for 24 hours. The swollen samples were then vacuum-dried at 100°C at 1 torr for 24 hours, until no further mass change from solvent evaporation was measurable.

Characterization by Differential Scanning Calorimetry

Differential scanning calorimetry (DSC) was used to determine if crystallinity was present in the samples and also to determine the glass transitions of the materials. Experiments were run using a Perkin–Elmer Diamond DSC. 5 mg samples were cut from heat and radiation-crosslinked samples and placed in standard aluminum DSC pans. The samples were loaded at room temperature. The temperature range was −20–200°C, with a ramp rate of 20°C/min and a soak time of 2 min at the end of each heating/cooling cycle. An initial ramp cycle was run for each sample to relieve thermal stress and allow any residual solvent or monomer to evaporate, and a second ramp cycle was run to determine T_g. Glass transitions were determined using the Pyris software according to the half-height method.

Characterization by Dynamic Mechanical Analysis

DMA experiments were run on all samples subjected to heating or irradiation using a TA Instruments DMA Q800 Series dynamic mechanical analyzer controlled by a PC running Q Series software. Test samples were cut from 1mm-thick films to 5mm × 12 rectangles.

DMA Isostrain Tests—In order to determine if samples were crosslinked, and also to determine storage modulus and T_g, the samples were subjected to DMA isostrain tests. In the “DMA Multifrequency-Strain” mode, frequency was set to 1.0 Hz, strain was set to 0.1%, preload force was set to 0.01 N, and forcetrack was set to 125%. The temperature range was 0–200 °C with a ramp rate of 5°C/min. If sample slippage occurred during the glass transition, the ramp rate was slowed to 2°C/min over the range of $T = T_g \pm 10°C$, and the sample was re-run. Plots of storage modulus and tan delta versus temperature were recorded using the QSeries software. T_g was determined from the peak of the tan delta curves.

Cyclic Free Strain Recovery Tests—Cyclic free strain recovery experiments were run in tension to evaluate the difference in percent recoverable strain between the thermoplastic and crosslinked samples. In the “DMA- Strain Rate” mode, frequency was set to 1.0 Hz, strain was set to 1.5%, and preload force was set to 0.01 N. The samples were heated to 35°C above T_g (tan delta peak), strained to 50%, and were then rapidly quenched to 0°C at −10°C/min while maintaining the 50% strain. Then, for free-strain recovery, the applied force was set to 0N, and the temperature was ramped from 0°C to 140°C at 5°C/min. For cyclic testing, the samples were cooled back to $T_g + 35°C$ at −10°C/min, strained again to 50%, and the previous procedures were repeated. Percent strain recovered as a function of temperature and time was recorded using the QSeries software. For thermoplastic samples, 2-cycle experiments were run, and for crosslinked samples, 3-cycle experiments were run.

Constrained Recovery Tests—In order to determine the maximum recovery stress of the samples in the new urethane system and evaluate the effect of crosslinking on recovery stress, constrained recovery tests were run on samples 1a and 1R-a. Sample 1R-a was chosen because it had the highest overall rubbery modulus value at $T = T_g + 20°C$. In the "DMA- Strain Rate" mode, frequency was set to 1.0 Hz, strain was set to 1.0 %, and preload force was set to 0.01 N. The samples were heated to 75°C, strained to 50%, and were then rapidly quenched to 0°C at −10°C/min while maintaining the 50% strain. Finally, the samples were heated from 0°C to 150°C at 5°C/min without removing the applied stress. Recovery stress was recorded as a function of temperature.

Characterization by Tensile Testing

To determine toughness values, ultimate tensile strengths, and failure strains, tensile testing was carried out on Series 1H. Dog bone samples were cut using a CO_2 laser according to ASTM Standard D-412. Strain to failure experiments were run three times on each sample using 100N load cell in a TA Instruments Insight 2® tensile testing machine. Experiments were run at T_g, which was determined from the peak of the tan deltas from DMA plots.

Characterization by Qualitative Shape Recovery Analysis

Recovery time was measured using qualitative shape recovery analysis. The qualitative recovery analysis was performed on Samples 1R-a and 1H-a, which had sharper glass transition curves than any other materials with T_g's within 5°C of body temperature. In these tests, flat 4 × 60 × 1 mm samples were coiled into helical shapes at 70°C. The deformed samples were then quenched by immersion in an ice water bath to maintain the helical shapes. The samples were then placed in 37°C water, and the shape recovery was recorded using a high-definition digital video camera.

RESULTS AND DISCUSSION

Swelling studies and DMA results showed that several of the new urethane systems were crosslinked. Mechanical characterization revealed that the materials had mechanical properties highly suitable for biomedical applications.

Solvent Swelling Results

While the 1H thermally crosslinked urethanes all had gel fractions above 90%, the 1R radiation crosslinked urethanes showed a significant decrease in gel fraction as DCHMDI composition was increased from 0–30%. A plot of chemical composition versus percent gel fraction for Series 1H and 1R is provided in Figure 2. Swelling data for all samples is provided in Table 2.

Since the 2-butene-1,4-diol was only 95% pure, and since the urethane samples may have absorbed moisture from the atmosphere before solvent evaporation, the evaporation of water and other impurities may have made the gel fractions appear even lower than they actually were. Thus, the gel fraction results from the thermally crosslinked urethanes (and any other gel fractions above 90%) are strong evidence of chemical crosslinking.[22]

DSC Results

DSC results for Series I samples are provided in Figure 3, and are representative of the behavior of all samples. These results show a single step transition indicative of a glass transition, with no indication of crystallinity or other secondary phases. The glass transitions range from 29 to 73 °C. Since SMPs in the state of their secondary geometries begin shape-recovery at T_g, it is important that SMP-based biomedical implant devices have glass

transitions above room temperature in order to maintain their secondary shapes at room temperature. The T_g of Sample 1H-a was 29°C, which is above room temperature, suggesting it should be suitable for biomedical applications.

DMA Results

DMA Isostrain Results—DMA results on all heated and certain irradiated samples are shown in Figures 4–9. All samples showed curves characteristic of amorphous polymers, i.e., a glassy region at low temperatures, a glass transition at higher temperatures, and a rubbery plateau. Figure 4 compares the DMA curves for thermoplastic, radiation crosslinked, and thermally crosslinked 1a samples. These plots show significant changes in the rubbery modulus values before and after heating and irradiation. While the thermoplastic sample 1a melts around 120 °C, the irradiated and heated samples do not flow at temperatures well above T_g; this behavior indicates that significant crosslinking has occurred.

Figure 5, a comparison of storage modulus plots for all thermally crosslinked samples, shows the polymers to have glass transitions from 32 to 80°C and rubbery moduli from 1.9 to 4.0 MPa. The rubbery moduli for the samples remain constant and even increase slightly with increasing temperature, thus indicating ideal elastomeric behavior. In Figure 6, the tan deltas approach zero both above and below T_g. These figures show no additional transitions, such as those caused by crystalline melting. The sharpness of the glass transition, as seen in the tan delta curves, is evidence of a homogenous network structure. This homogeneity arises from the base polymer's being an alternating copolymer and is indicative that there is a narrow dispersion of molecular weights between crosslink sites.[23–25] When coupled with the high gel fraction data listed in Table 2 and displayed in Figure 2, the DMA results in Figures 4–6 provide decisive evidence that the samples in Series 1H are chemically crosslinked.

The thermal crosslinking mechanism was studied by evaluating the effects of temperature and heat exposure time on crosslinking. As indicated by the storage modulus plots in Figure 7, increased heat exposure time increased the extent of thermal crosslinking. Increasing the temperature also accelerated the crosslinking process, as is illustrated by the storage modulus plot for Sample 5a. This sample had a positive-sloping rubbery modulus of 0.4 MPa, after heating to 225°C for only 2.5 hours. Although elastic behavior was seen to increase with heat exposure time for the 200°C samples, none of these samples became adequately crosslinked in the 10-hr time period shown in Figure 7.

Storage modulus plots for Samples 1R-a, 1R-c, 1R-d, and 1R-e are plotted together in Figure 8. These plots show the effect of increasing DCHMDI composition on radiation crosslinking. As evidenced by the gel fraction results in Figure 2, the DMA tests indicated that the DCHMDI monomer inhibited radiation crosslinking. The plots in Figure 8 follow the same trend as the gel fraction results in Figure 2: increasing DCHMDI composition again resulted in more thermoplastic behavior (less crosslinking).

In order to evaluate the effect of the unsaturated group in 2-butene-1,4-diol on radiation crosslinking, Sample 1R-f, made from the saturated 1,4-butanediol monomer, was characterized and compared to sample 1R-a, which was made from 2-butene-1,4 diol. The only difference between these two monomers was the existence of the unsaturated group in 2-butene-1,4-diol. As seen in Figure 9, a comparison of the storage moduli of the two samples, the rubbery modulus of Sample 1R-a at T_g + 20°C was 4.2 MPa, while that of the saturated 1f-R sample was 0.2 MPa.

Furthermore, as shown in Table 2, the gel fraction of the 1,4-butanediol was only 78.8%, while that of the 2-butene-1,4-diol sample was 93.3%. Thus, some crosslinking did occur in Sample 1R-f, as predicted by past urethane studies. However, the double bond adjacent to the ester α-hydrogen appears to facilitate crosslinking.

Cyclic Free Strain Recovery Results—Percent recoverable strain was determined during free recovery over repeated cycles. Figure 10 compares the free strain recovery for thermoplastic and thermally crosslinked 20% DCHMDI samples. After the first cycle, the thermally crosslinked sample recovered 95.5% strain. After the second and third cycles, the sample recovered 94.8% and 94.6% strain, respectively. The thermoplastic samples did not demonstrate high percent recoverable strain. After cycle 1, percent recoverable strain was 46.1%, and after cycle 2, it was 3.1%. Cyclic free strain recovery plots are shown for thermally crosslinked and thermoplastic 20% DCHMDI samples in Figures 10(a) and (b), respectively.

Constrained Recovery Results—The radiation crosslinked 0% DCHMDI sample was subjected to constrained recovery testing because it had the highest rubbery modulus (4.2 MPa) at $T = T_g + 20°C$ of any sample characterized in this work. Figure 11 compares the constrained recovery results for the thermoplastic and radiation crosslinked samples. At body temperature (37°C), the recoverable stress of the crosslinked sample was 0.66MPa (95 PSI), and its maximum recoverable stress was 0.83MPa (121 PSI). The thermoplastic sample did not exhibit a recoverable stress.

Tensile Testing Results

Strain to failure showed the new urethanes to have high toughness. Figure 12 shows the average strain/strain data for three successful strain to failure experiments on Sample 1H-d, 20% DCHMDI. All three samples strained to over 500% elongation, while still exhibiting significant strain hardening. Toughness was calculated to be 50.2 MJ/m^3.

Qualitative Shape -Recovery Analysis Results

The coiled samples both achieved full shape recovery in 12 seconds at body temperature. Images of Sample 1R-a at different points in its 12-second recovery period are provided in Figure 15 (1H-a was tested, but is not pictured). Each sample was deformed into the coiled shape shown at time 0 in Figure 13 and put in water at 37°C.

DISCUSSION

The primary objective of this work was the synthesis and characterization of a novel shape-memory polymer that could be synthesized into a thermoplastic, processed into a complex geometry using injection molding, and later crosslinked in a secondary step. The DMA plots in Figures 4–8, cyclic free strain recovery comparisons in Figure 10, and constrained recovery comparisons in Figure 11 are evidence of both the existence of chemical crosslinking and of its effects on the mechanical properties of the SMP systems. The fact that all the materials in these plots had over 90% gel fractions is further confirmation that chemical crosslinking occurred.

From the characterization of the radiation-induced crosslinking mechanism attempted in this work, several conclusions could be drawn. First, the DCHMDI-containing samples did not appear suitable for radiation crosslinking at room temperature. One explanation for the DCHMDI monomer's inability to undergo radiation crosslinking is that the DCHMDI molecules in the polymer backbone experienced chain scission during irradiation, which prevented the formation of a large network structure. DCHMDI contains two cyclohexyl

groups, which induce high stiffness on the polymer chains and therefore increase T_g. Because DCHMDI-containing samples have glass transitions significantly above room temperature, chain mobility is limited, and the probability that radical-containing chains will interact via radical graft polymerization to form crosslinks is decreased. The gel fractions of the DCHMDI-containing samples decreased proportionally with increasing T_g, as indicated in Table 2.

Second, the 2-butene-1,4-diol monomer appears to be ideal for radiation crosslinking. A proposed radiation crosslinking mechanism for the urethane is provided in Figure 14. Previous research[26–29] has shown that e -beam radiation can cause crosslinking in polyurethanes by ionizing the α-hydrogen adjacent to the carbamate oxygen in the urethane backbone and initiating a radical-based “graft” polymerization (instead of a radical chain polymerization), where radicals on different carbons form one-to-one chain-linking covalent bonds. [30–31] The chemical structure of the thermoplastic urethane (Sample 1a) is provided in Figure 14 (Structure I), and the α-hydrogens are shown in bold. What is unique about this urethane is that the α-hydrogens are adjacent to the double bond from the 2-butene-1,4-diol monomer. Consequently, when the radiation-induced radicals form, the radicals theoretically experience extended resonance stabilization along parts of the alcohol segment and through the carbamate linkages of the polymer backbone. We have proposed two possible resonance structures, which are Structures II and III in Figure 14. This extended resonance stabilization gives the radicals more time to bond to other radicals and consequently increases crosslinking. The fact that the 1,4-butanediol sample, 1f-R, had both a lower rubbery modulus at $T = T_g + 20°C$ and a lower gel fraction than its unsaturated counterpart indicates that the unsaturated group is involved in the crosslinking mechanism. The comparison of the storage modulus plots for Samples 1a-R and 1f-R in Figure 9 illustrates this point.

A characterization of the thermal crosslinking mechanism was attempted by examining the relationship between temperature and heat exposure time on crosslinking. Figure 6 shows that both increased heat exposure time and increased temperature increased the thermal crosslinking. However, most of the rubbery modulus values in Figure 6 are too low for the corresponding materials to be considered thermoset SMPs, and further analysis of the thermal crosslinking mechanism is necessary before quantitative conclusions can be drawn about the mechanism.

In addition to the gel fraction tests and DMA experiments, one final experiment was run in order to determine if the objective of creating a polyurethane SMP that could be processed as a thermoplastic and then subsequently crosslinked had been met. Sample 1A was molded into the geometry of a complex medical device, pictured in Figure 15. This device, an artificial oropharyngeal airway device, was exposed to radiation, during which it underwent radiation-induced chemical crosslinking, and after which it was shown to exhibit shape-memory properties. Qualitative shape-recovery experiments were again run on the actual SMP-based airway device, and full recovery occurred in 14 seconds at body temperature.[32]

In conclusion, this project met and exceeded its objectives. Novel post-condensation crosslinked polyurethane shape-memory polymers were synthesized, characterized, and injection molded into the geometry of a complex medical device. Mechanical characterization results revealed that these materials have mechanical properties that are ideal for many biomedical applications. As a result of the work done in this project, the mass-production of complex SMP-based devices, which has historically been significantly limited, may become more economically feasible.

CONCLUSIONS

1. In this work, a series of novel polyurethane shape-memory polymers was successfully developed that can be first made into thermoplastic precursors and later crosslinked in a secondary step. These new materials were determined to have outstanding mechanical properties. Such properties include a T_g range of 32–80°C, a rubbery modulus range of 0.1–4.2 MPa, a maximum recoverable stress of 0.83 MPa, cyclic recoverable strains approaching 100%, and a shape-recovery time of 12 seconds at body temperature.
2. These new polyurethanes can be crosslinked either by heat or electron beam irradiation. A characterization of both the radiation-induced and thermally-activated crosslinking mechanisms utilized in this work was attempted. The DCHMDI monomer appeared to inhibit radiation crosslinking because of chain mobility restriction, and the 2-butene-1,4-diol monomer appeared to enhance radiation crosslinking because of resonance stabilization of radiation-induced radicals. Both increased temperature and increased time of heat exposure increased the degree of thermal crosslinking.
3. Based on the aforementioned properties and demonstration of an injection molded complex medical device, these materials appear to have potential in a variety of medical device applications.

Acknowledgments

This work was partially performed under the auspices of the U.S. Department of Energy by Lawrence Livermore National Laboratory under Contract DE-AC52-07NA27344 and supported by the National Institutes of Health/ National Institute of Biomedical Imaging and Bioengineering Grant R01EB000462.

References

1. Yakacki CM, Shandas R, Lanning C, Rech B, Eckstein A, Gall K. Biomaterials. 2007; 28:2255. [PubMed: 17296222]
2. Small W, Wilson TS, Maitland D. J Optics Express. 2005:13.
3. Metzger MF, Wilson TS, Schumann D, Matthews DL, Maitland DJ. Biomedical Microdevices. 2002; 4:89.
4. Gall K, Kreiner P, Turner D, Hulse M. Microelectromechanical Systems, Journal of. 2004; 13:472.
5. Maitland DJ, Metzger MF, Schumann D, Lee A, Wilson TS. Lasers in Surgery and Medicine. 2002; 30:1. [PubMed: 11857597]
6. Sanderson T, Gall K. Raytheon Technology Today. 2007; 10:10.
7. Lendlein A, Langer R. Science. 2002; 296:1673. [PubMed: 11976407]
8. Gall K, Yakacki CM, Liu Y, Shandas R, Willett N, Anseth KS. Journal of Biomedical Materials Research Part A. 2005; 73A:339. [PubMed: 15806564]
9. FDA. in FDA Medical Devices; Services, U. S. D. o. H. a. H., Ed.: 2009.
10. DiPrima MA, Lesniewski M, Gall K, McDowell DL, Sanderson T, Campbell D. Smart Materials and Structures. 2007; 16:2330.
11. Behl M, Lendlein A. Materials today. 2007:10.
12. Liu C, Qin H, Mather PT. Journal of Materials Chemistry. 2007:17.
13. Davis KA, Burdick JA, Anseth KS. Biomaterials. 2003; 24:2485. [PubMed: 12695075]
14. Yakacki CM, Shandas R, Safranski D, Ortega AM, Sassaman K, Gall K. Advanced Functional Materials. 2008; 18:2428. [PubMed: 19633727]
15. Hu J, Yang Z, Yeung L, Ji F, Liu Y. Polymer International. 2005; 54:854.
16. Hosler D, Burkett SL, Tarkanian MJ. Science. 1999; 284:1988. [PubMed: 10373117]

17. Le Roy, P. M. B., FR), Pattein, Jacky P. (Etrechy, FR). Societe Nationale des Poudres et Explosifs (Paris, FR), United States: 1982.
18. Goyert, W. L., DE), Winkler, Jurgen (Leverkusen, DE), Perrey, Hermann (Krefeld, DE), Heidingsfeld, Herbert (Frechen, DE). Bayer Aktiengesellschaft (Leverkusen, DE), United States: 1988.
19. Bezuidenhout, D. C. T., ZA), Theron, Jacobus P. (Stellenbosch, ZA), Higham, Lawrence J. (Durbanville, ZA), Zilla, Peter P. (Cape Town, ZA). Medtronic, Inc. (Minneapolis, MN, US), United States: 2009.
20. Voit W, Ware T, Dasari RR, Smith P, Danz L, Simon D, Barlow S, Marder SR, Gall K. Advanced Functional Materials. 2010; 20:162.
21. Ware T, Voit W, Gall K. Radiation Physics and Chemistry. 2010; 79:446.
22. Park SH, Kim JW, Lee SH, Kim BK. Journal of Macromolecular Science, Part B: Physics. 2005; 43:447.
23. Hu JL, Ji FL, Wong YW. Polymer International. 2005; 54:600.
24. Lendlein A, Schmidt AM, Schroeter M, Langer R. Journal of Polymer Science Part A: Polymer Chemistry. 2005; 43:1369.
25. Liu Y, Gall K, Dunn ML, Greenberg AR, Diani J. International Journal of Plasticity. 2006; 22:279.
26. Clough RL. Nuclear Instruments and Methods in Physics Research Section B: Beam Interactions with Materials and Atoms. 2001; 185:8.
27. Majumder PS, Bhowmick AK, Majali AB, Tikku VK. Journal of Applied Polymer Science. 2000; 75:784.
28. Zhu G, Liang G, Xu Q, Yu Q. Journal of Applied Polymer Science. 2003; 90:1589.
29. Zhu GM, Xu QY, Liang GZ, Zhou HF. Journal of Applied Polymer Science. 2005; 95:634.
30. Wall LA. Journal of Polymer Science. 1955; 17:141.
31. Vijayabaskar V, Bhattacharya S, Tikku VK, Bhowmick AK. Radiation Physics and Chemistry. 2004; 71:1045.
32. Ware, T. H., K. Simon, D. Sassaman, K. Gall, K., Materials, A. S. o., Ed. Atlanta, GA: 2009.

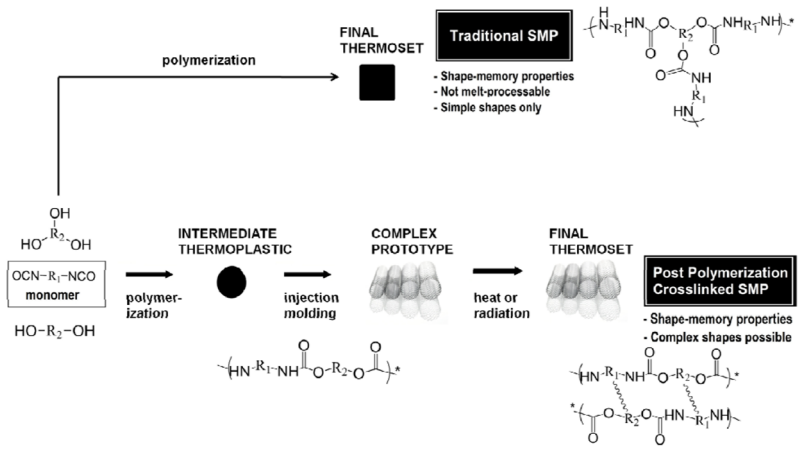

Figure 1.
Comparison of synthesis and processing of a traditional SMP and a post-condensation crosslinked SMP

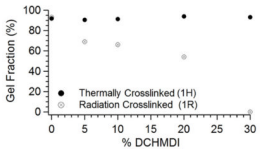

Figure 2.
Plots of gel fraction versus % DCHMDI for 1H and 1R series.

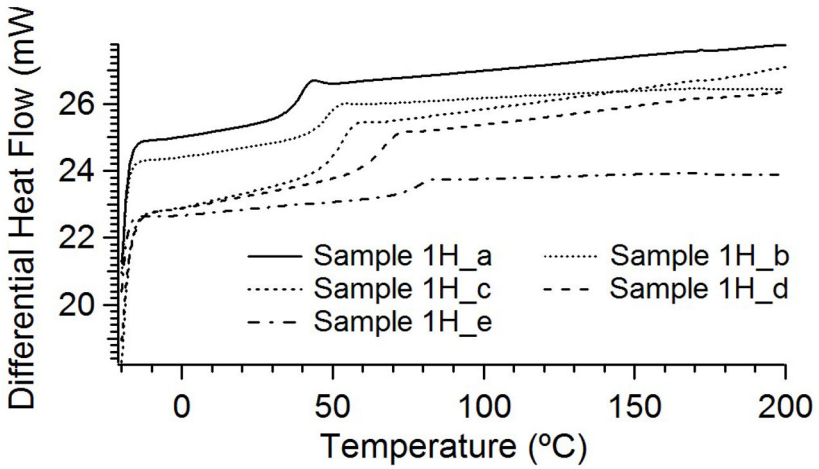

Figure 3.
DSC results for Series 1 thermally crosslinked samples

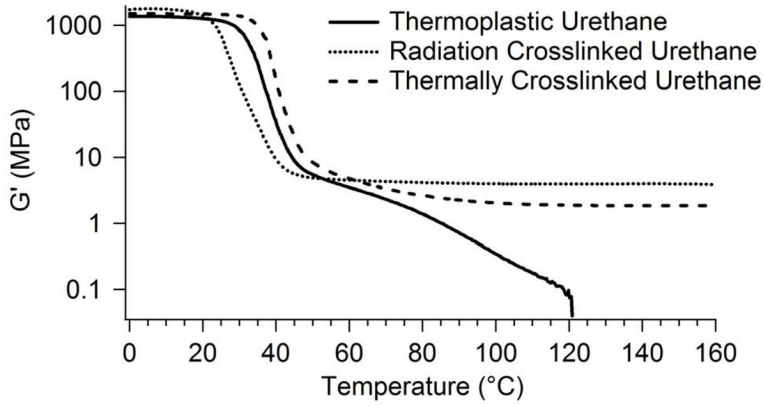

Figure 4.
Storage modulus plots for thermoplastic, radiation crosslinked, and heat crosslinked 1-a urethane sample

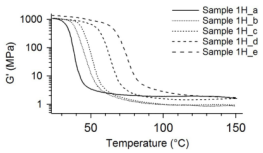

Figure 5.
DMA storage modulus (G′) plots for thermally crosslinked samples in Series 1H

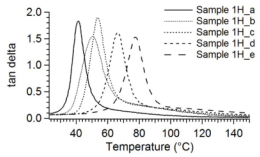

Figure 6.
Tan delta plots for thermally crosslinked samples in Series 1H

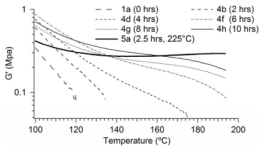

Figure 7.
Effect of heating time and temperature on rubbery modulus of Series 4 and 5 samples.

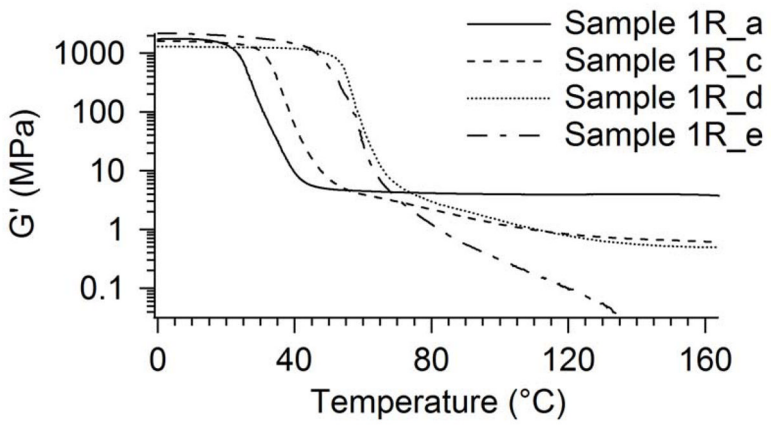

Figure 8.
Effect of Increasing DCHMDI composition on radiation crosslinking of select samples in Series 1R

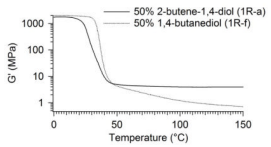

Figure 9.
A comparison of the storage moduli of samples 1a-R (radiation crosslinked 50% 2-butene-1,4-diol sample) and 1f-R (50% 1,4-butanediol)

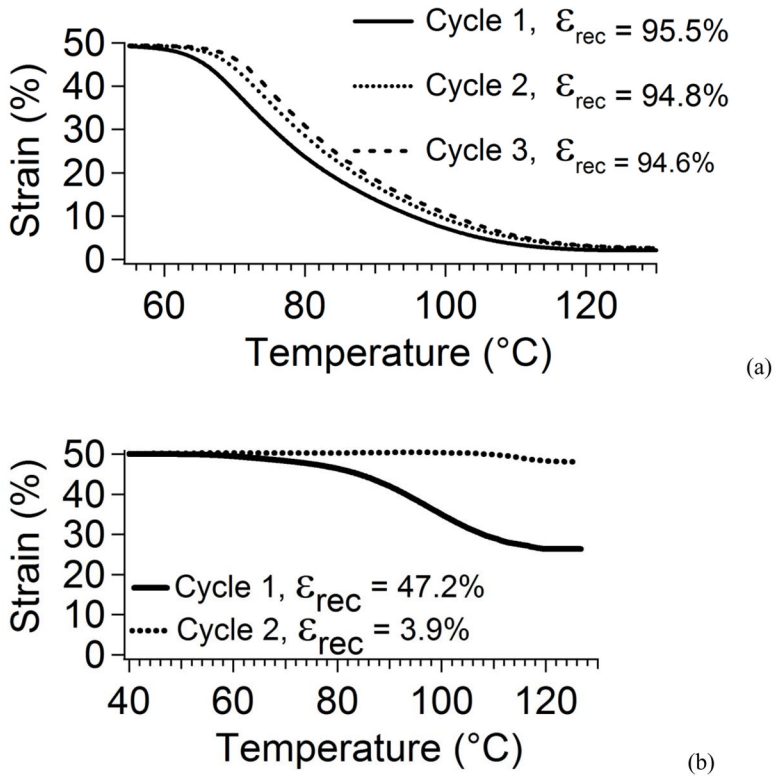

Figure 10.
Cyclic Free strain recovery plots of recovered strain versus temperature for (a) thermally crosslinked 20% DCHMDI sample and (b) thermoplastic 20% DCHMDI sample

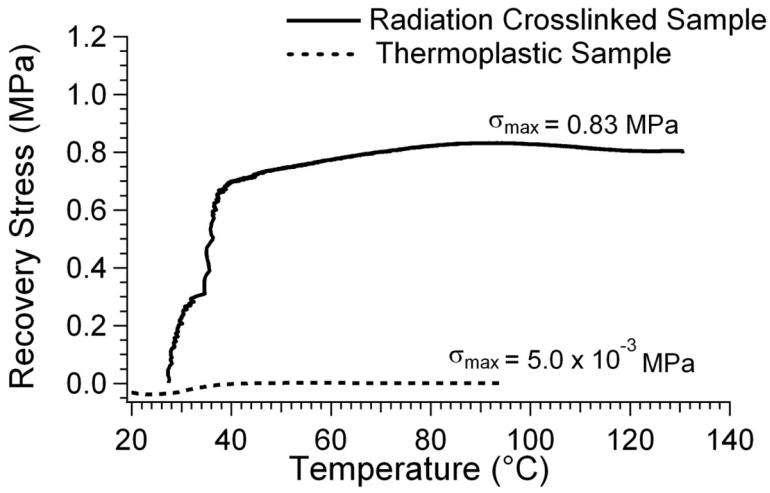

Figure 11.
Constrained recovery plot of recoverable stress versus temperature for thermoplastic and radiation crosslinked (1R_a) 0% DCHMDI sample.

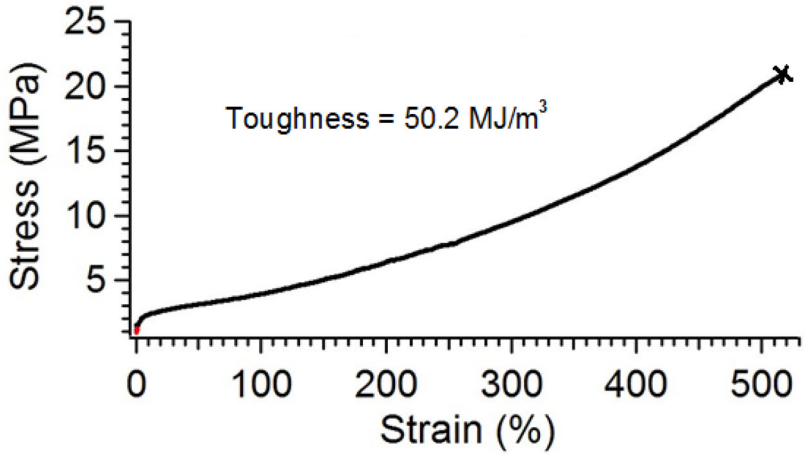

Figure 12.
Strain to Failure Results for Sample 1H-d

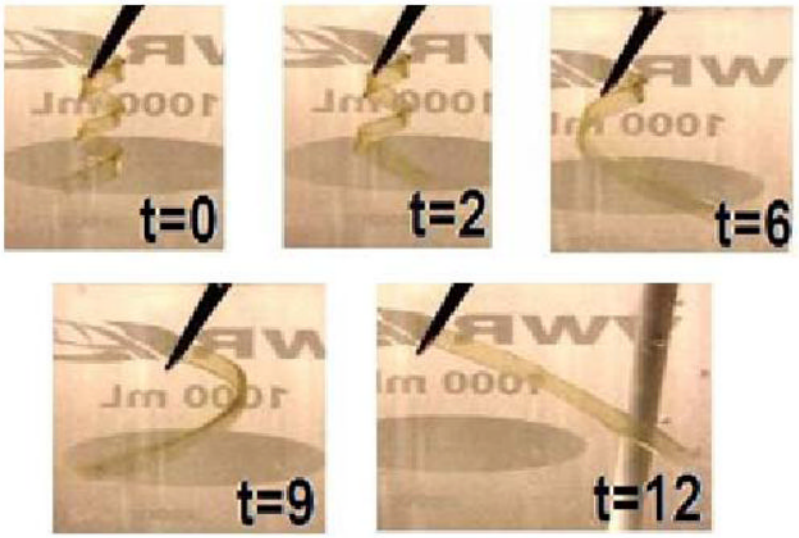

Figure 13.
Images of the shape recovery at 37°C of sample 1R_a over a 12-second time period.

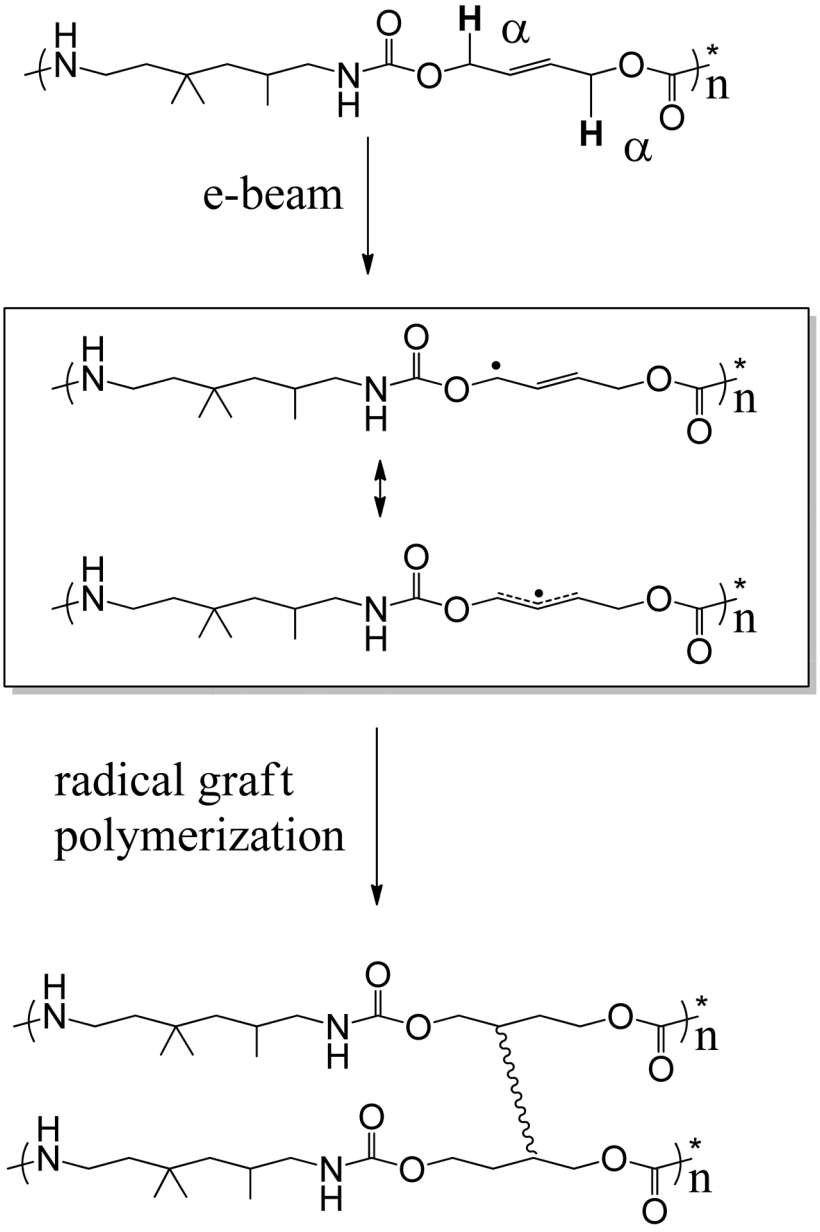

Figure 14.
Proposed chemical mechanism for the radiation crosslinking of samples containing 2-butene-1,4-diol

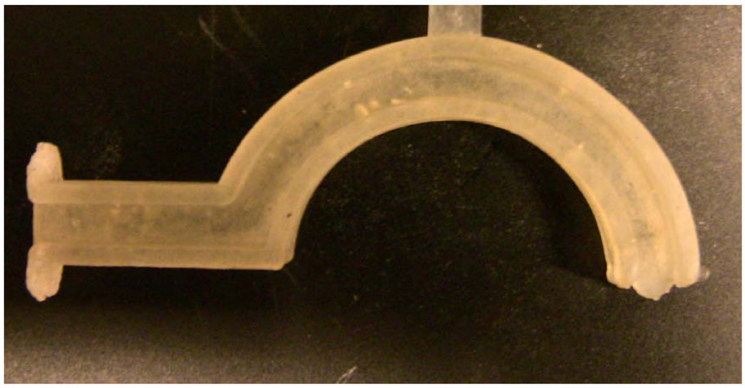

Figure 15.
Artificial oropharyngeal airway device made from molding Sample 1a and then exposing it to radiation

Table 1

Compositions of Series 1, 1R, 1H, 2, 2R, 3, and 3R samples. Chemical structures of monomers are included

Series 1, 1H, 1R	DCHMDI	TMHDI	Un-crosslinke	Heat Crosslinked	Radiation Crosslinked	Chemical Structures
	0%	50%	1a	1H-a	1R-a	Diols
	5%	45%	1b	1H-b	1R-b	2-butene-1,4-diol
	10%	40%	1c	1H-c	1R-c	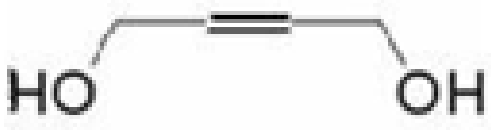
50% 2-butene-1,4-diol	20%	30%	1d	1H-d	1R-d	
	30%	20%	1e	1H-e	1R-e	1,4 butanediol
50% 1,4 butanediol	0%	50%	1f	-	1R-f	
Series 2, 2R	**1, 8-octanediol**	**2-butene-1,4-diol**				1,6 hexanediol 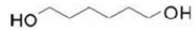
	5%	45%	2a	-	2R-a	
	15%	35%	2b	-	2R-b	1,8 octanediol
50% TMDHI	20%	30%	2c	-	2R-c	
	25%	25%	2d	-	2R-d	Diisocyanates
Series 3, 3R	**1,6-hexanediol**	**2-butene-1,4-diol**				TMHDI 
	10%	40%	3a	-	3R-a	
	15%	35%	3b	-	3R-b	DCHMDI
50% TMHDI	20%	30%	3c	-	3R-c	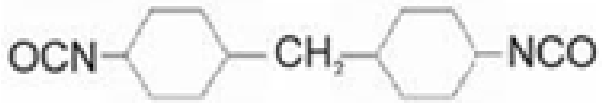
	25%	25%	3d	-	3R-d	

Table 2

Solvent swelling results for all samples

Sample	Gel Fr.	Sample	Gel Fr.	Sample	Gel Fr.
1H_a	91.8%	1R_a	93.2%	2R_b	80.2%
1H_b	90.5%	1R_b	68.9%	2R_d	95.8%
1H_c	91.3%	1R_c	66.1%	3R_c	72.2%
1H_d	93.9%	1R_d	54.0%	1R_f	78.8%
1H_e	93.3%	1R_e	0.0%		